Cancer Chemother Pharmacol (2001) 47: 385–390
DOI 10.1007/s002800000256

ORIGINAL ARTICLE

**Stacey Berg · Baruti Serabe · Aleksander Aleksic
Lisa Bomgaars · Leticia McGuffey · Robert Dauser
John Durfee · Jed Nuchtern · Susan Blaney**

Pharmacokinetics and cerebrospinal fluid penetration of phenylacetate and phenylbutyrate in the nonhuman primate

Received: 21 July 2000 / Accepted: 16 November 2000 / Published online: 16 February 2001

Abstract *Introduction:* Phenylbutyrate (PB) and its metabolite phenylacetate (PA) demonstrate anticancer activity in vitro through promotion of cell differentiation, induction of apoptosis through the p21 pathway, inhibition of histone deacetylase, and in the case of PB, direct cytotoxicity. We studied the pharmacokinetics, metabolism, and cerebrospinal fluid (CSF) penetration of PA and PB after intravenous (i.v.) administration in the nonhuman primate. *Methods:* Three animals received 85 mg/kg PA and 130 mg/kg PB as a 30-min infusion. Blood and CSF samples were obtained at 15, 30, 35, 45, 60 or 75 min, and at 1.5, 2.5, 3.5, 5.5, 6.5, 8.5, 10.5 and 24.5 h after the start of the infusion. Plasma was separated immediately, and plasma and CSF were frozen until HPLC analysis was performed. *Results:* After i.v. PA administration, the plasma area under the concentration-time curve (AUC) of PA (median ± SD) was 82 ± 16 mg/ml·min, the CSF AUC was 24 ± 7 mg/ml·min, clearance (Cl) was 1 ± 0.3 ml/min per kg, and the AUC_{CSF}:AUC_{plasma} ratio was 28 ± 19%. After i.v. PB administration, the plasma PB AUC was 19 ± 3 mg/ml·min, the CSF PB AUC was 8 ± 11 mg/ml·min, the PB Cl was 7 ± 1 ml/min per kg, and the AUC_{CSF}:AUC_{plasma} ratio was 41 ± 47%. The PA plasma AUC after i.v. PB administration was 50 ± 9 mg/ml·min, the CSF AUC was 31 ± 24 mg/ml·min, and the AUC_{CSF}:AUC_{plasma} ratio was 53 ± 46%. *Conclusions:* These data indicate that PA and PB penetrate well into the CSF after i.v. administration. There may be an advantage to administration of PB over PA, since the administration of PB results in significant exposure to both active compounds. Clinical trials to evaluate the activity of PA and PB in pediatric central nervous system tumors are in progress.

Key words Phenylacetate · Phenylbutyrate · Cerebrospinal fluid · Pharmacokinetics

Introduction

Phenylbutyrate (PB) and its metabolite phenylacetate (PA) are aromatic fatty acids that are currently undergoing clinical investigation for their antitumor and differentiating effects. PB undergoes rapid and nearly complete capacity-limited (nonlinear) metabolism to PA in vivo [1]. PA, a deaminated metabolite of phenylalanine, is normally present in the mammalian circulation in micromolar concentrations [2]. PA is eliminated by conjugation with glutamine to yield phenylacetylglutamine (PAG) which is then excreted in the urine [3, 4]. In children with hyperammonemia due to inborn errors of urea synthesis, PA is administered in pharmacologic doses (grams of drug per kilogram of body weight) and mobilization of glutamine-associated nitrogen is believed to lead to the observed improvements in hyperammonemia [5, 6].

In preclinical studies, exposure to millimolar concentrations of PA or PB in vitro can induce tumor cytostasis and differentiation in a variety of tumor cell lines, including malignant gliomas, hormone-refractory prostate carcinoma, malignant melanoma, neuroblastoma, lymphoblastic leukemia, and adenocarcinomas of the breast, colon and lung [7, 8, 9, 10, 11, 12, 13, 14, 15, 16, 17]. Among the postulated mechanisms for the cytostatic and differentiating effects of PA and PB are alterations in lipid metabolism, regulation of gene expression through DNA hypomethylation and transcriptional activation, inhibition of protein isoprenylation, and glutamine depletion [10]. Recently, PB has also been implicated in inhibition of histone deacetylase

This work was supported in part by the Clayton Foundation for Research.

S. Berg (✉) · B. Serabe · A. Aleksic · L. Bomgaars
L. McGuffey · R. Dauser · J. Durfee · J. Nuchtern · S. Blaney
Texas Children's Cancer Center and Texas Children's Hospital,
Baylor College of Medicine, Houston, TX, USA

Correspondence address:
S. Berg
Texas Children's Cancer Center,
6621 Fannin St., MC3-3320, Houston TX 77030, USA
E-mail: sberg@txccc.org; Tel.: +1-832-824-4588

activity [18, 19]. These unusual mechanisms of action, combined with preclinical evidence of antitumor activity, have led to the clinical development of PA and PB as potential anticancer agents.

We studied the pharmacokinetics of PA and PB in a nonhuman primate model that is highly predictive of the central nervous system (CNS) penetration of anticancer drugs in humans [20].

Methods

Animals

Three adult male Rhesus monkeys (*Macaca mulatta*) weighing 10.0–11.6 kg were used for this study. The animals were fed High Protein Monkey Diet No. 5045 (Lab Diet, St Louis, Mo.), and were group-housed in accordance with the Guide for the Care and Use of Laboratory Animals [21]. Blood samples were drawn from a catheter placed in either the internal jugular vein or the saphenous vein. Cerebrospinal fluid (CSF) samples were drawn from a subcutaneous Ommaya reservoir attached to an indwelling Pudenz catheter, with the tip located in the fourth ventricle. As previously described, this model permits drug infusion and repeated blood and CSF sampling in unanesthetized animals [20].

Drugs

PA and PB were generously supplied by Targon Corporation (Princeton, N.J.). PAG for HPLC standards was supplied by Elan Pharmaceutical and Research Company (Gainesville, Ga.).

Animal experiments

Sodium PA (85 mg/kg) was administered as a 30-min intravenous (i.v.) infusion to three animals. In separate experiments sodium PB (130 mg/kg) was administered as a 30-min infusion to the same animals. Blood and CSF samples were obtained at 15, 30, 35, 45, 60 or 75 min, and at 1.5, 2.5, 3.5, 5.5, 6.5, 8.5, 10.5 and 24.5 h after the start of the infusion. Plasma was separated immediately, and plasma and CSF were frozen until HPLC analysis was performed.

HPLC analysis

PB, PA, and PAG were measured using high-pressure liquid chromatography [22]. In brief, 200 µl plasma was deproteinized by the addition of 20 µl 40% $ZnSO_4$ and 180 µl methanol followed by centrifugation for 10 min at 16,000 *g*. A 20-µl aliquot of supernatant was then injected into the HPLC system, which consisted of a Model 717 Plus autosampler, a Model 600E Multisolvent Delivery System, and a Model 996 photodiode array detector (Millipore Corporation, Waters Chromatography, Milford, Mass.). Samples were separated using a Nova-pack C18 3.9 × 300 mm, 4 µm analytical column with a Nova-pack C18, C3.9 × 20 mm, 4 µm guard column heated to 60°C. The mobile phase consisted of a step gradient of 16% acetonitrile/84% 5 m*M* phosphoric acid from 0 to 1 min, 50% acetonitrile/50% 5 m*M* phosphoric acid from 1 to 11 min and 16% acetonitrile/84% 5 m*M* phosphoric acid from 11 to 20 min. Absorbance was measured at 208 nm. Retention times were 5.0 min for PAG, 9.5 min for PA, and 11.5 min for PB. The limit of quantitation was 0.1 µg/ml for PA, 0.15 µg/ml for PB, and 0.3 µg/ml for PAG.

Pharmacokinetic analysis

Pharmacokinetic parameters were calculated using model-independent methods. The terminal rate constant (λ) was determined by linear regression through the time-points on the terminal portion of the elimination curve. The terminal half-life was calculated from the equation $t = 0.693/\lambda$. The AUC to the last time-point was measured by the trapezoidal method and the AUC was extrapolated to infinity (AUC_{inf}) by dividing the final concentration by λ. Clearance (Cl) was calculated as Cl = dose/AUC.

Subsequently, the model shown in Fig. 1 was fitted to the concentration-time data for all the experiments simultaneously using MLAB [23]. For infusion of PA, the compartments for PB in plasma and CSF were disregarded. In this model, the rate constants for transfer between compartments are indicated by k with the subscript indicating the compartments, Vmax represents the maximum rate of conversion of PA to PAG, Km is the Michaelis-Menten constant for conversion of PA to PAG, and V with a subscript represents the volume of the compartment indicated by the subscript. The volumes of the CSF compartments were fixed at 15 ml, the approximate CSF volume in Rhesus monkeys.

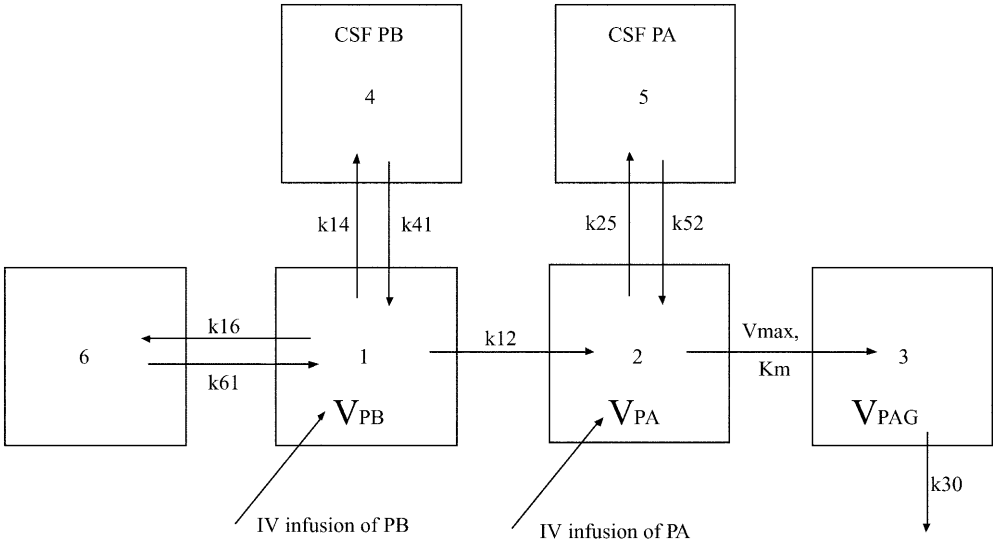

Fig. 1 Model for PB, PA and PAG in plasma and CSF after i.v. administration of PB or PA. The rate constants for transfer between compartments are indicated by *k* with the subscript indicating the compartments, *Vmax* represents the maximum rate of conversion of PA to PAG, *Km* is the Michaelis-Menten constant for conversion of PA to PAG, and *V* with a subscript represents the volume of the compartment indicated by the subscript

Results

Figure 2 shows plasma and CSF concentrations of PA and PAG in plasma and CSF after i.v. administration of PA. The pharmacokinetic parameters for PA after i.v. administration of PA are listed in Table 1. The plasma area under the concentration-time curve (AUC) for PA (median ± SD) was 82 ± 16 mg/ml·min, the CSF AUC was 24 ± 7 mg/ml·min, the clearance (Cl) was 1 ± 0.3 ml/min per kg, and the AUC_{CSF}:AUC_{plasma} ratio was 28 ± 19%. The terminal half-life of PA was 91 ± 37 min in plasma and 132 ± 47 min in CSF. The inactive metabolite PAG was also detected in plasma, with an AUC_{PAG}:AUC_{PA} ratio of 18 ± 11%.

Figure 3 shows PB, PA, and PAG in plasma (Fig. 3A) and CSF (Fig. 3B) after i.v. PB administration. The pharmacokinetic parameters for PB and PA after i.v. PB administration are listed in Tables 2 and 3. The plasma PB AUC was 19 ± 3 mg/ml·min, the CSF PB AUC was 8 ± 11 mg/ml·min, the PB Cl was 7 ± 1 ml/min per kg, and the AUC_{CSF}:AUC_{plasma} ratio was 41 ± 47%. The terminal half-life of PB was 19 ± 29 min in plasma and 127 ± 132 min in CSF. The PA plasma AUC after i.v. PB administration was 50 ± 9 mg/ml·min, the CSF AUC was 31 ± 24 mg/ml·min, and the AUC_{CSF}:AUC_{plasma} ratio was 53 ± 46%. The half-life of PA after i.v. PB administration was 70 ± 19 min in plasma and 197 ± 194 min in CSF. The AUC_{PA}:AUC_{PB} ratio was 234 ± 45% after i.v. PB administration. PAG was also detected after i.v. administration of PB, with an AUC_{PAG}:AUC_{PB} ratio of 90 ± 24% and an AUC_{PAG}:AUC_{PA} ratio of 40 ± 2%.

Table 4 shows the pharmacokinetic parameters derived from the model shown in Fig. 1. Although a model using only one compartment for PB was initially tried (results not shown), the data was best described by a two-compartment model for PB, with a linear rate constant describing the metabolism of PB to PA, a saturable (Michaelis-Menten) process describing the metabolism of PA to PAG, and linear transfer of PB and PA between plasma and CSF. The significance of the second compartment for PB, especially given the

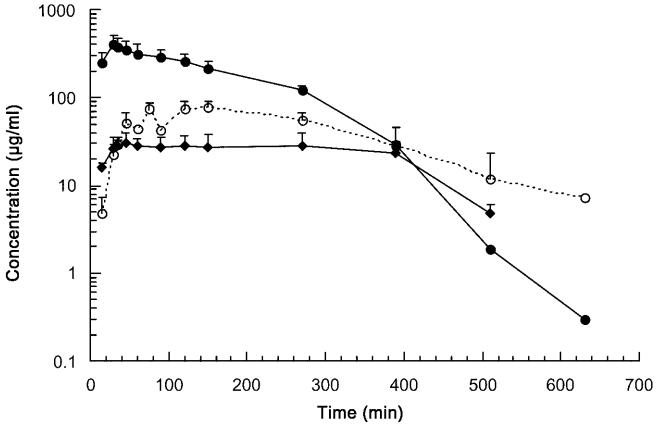

Fig. 2 PA (●) and PAG (◆) in plasma and PA in CSF (○) after an i.v. dose of 85 mg/kg PA ($n = 3$)

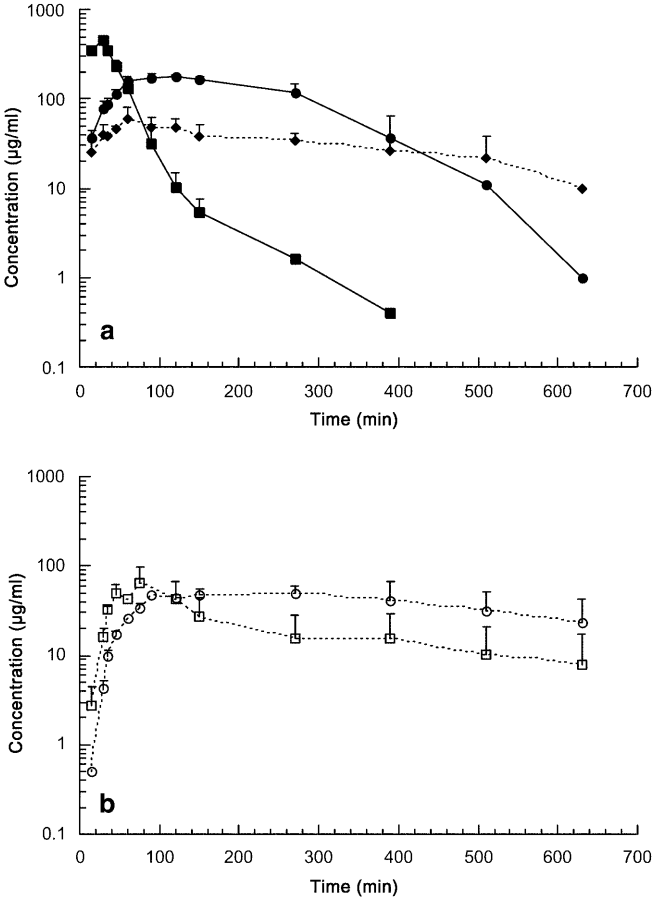

Fig. 3 **A** PB (■), PA (●), and PAG (◆) in plasma after an i.v. dose of 130 mg/kg PB ($n = 3$). **B** PB (□) and PA (○) in CSF after an i.v. dose of 130 mg/kg PB ($n = 3$)

Table 1 Pharmacokinetic parameters of PA in plasma and CSF after an i.v. dose of 85 mg/kg PA

Animal	Plasma AUC_{inf} (mg/ml·min)	Plasma half-life (min)	Clearance (ml/min/kg)	CSF AUC_{inf} (mg/ml·min)	CSF half-life (min)	AUC_{CSF}:AUC_{plasma}
1	82.0	98	1.05	19.4	132	0.24
2	84.8	91	1.02	23.7	67	0.28
3	56.2	30	1.50	33.3	159	0.59
Median	82.0	91	1.05	23.7	132	0.28
SD	15.7	37	0.27	7.1	47	0.19

Table 2 Pharmacokinetic parameters of PB in plasma and CSF after an i.v. dose of 130 mg/kg PB

Animal	Plasma AUC_{inf} (mg/ml·min)	Plasma half-life (min)	Clearance (ml/min/kg)	CSF AUC_{inf} (mg/ml·min)	CSF half-life (min)	AUC_{CSF}:AUC_{plasma}
1	17.3	16	7.5	6.1	85	0.36
2	23.1	19	5.6	27.6	332	1.20
3	19.4	68	6.7	8.0	127	0.41
Median	19.4	19	6.70	8.0	127	0.41
SD	3.0	29	0.95	11.9	132	0.47

Table 3 Pharmacokinetic parameters of PA in plasma and CSF after i.v. PB

Animal	Plasma AUC_{inf} (mg/ml·min)	Plasma half-life (min)	CSF AUC_{inf} (mg/ml·min)	CSF half-life (min)	AUC_{plasma}:AUC_{CSF}	AUC_{PA}:AUC_{PB} in plasma
1	40.4	70	14.9	106	0.37	2.3
2	49.8	87	61.1	479	1.23	2.2
3	58.2	49	30.9	197	0.53	3.0
Median	49.8	70	30.9	197	0.53	2.3
SD	8.9	19	23.5	194	0.46	0.4

Table 4 Pharmacokinetic parameters of PB and PA in plasma and CSF following i.v. PB or PA

Parameter	Value	Error
k_{12} (min^{-1})	0.0267	0.0071
k_{14} (min^{-1})	1.7×10^{-7}	2.17×10^{-8}
k_{16} (min^{-1})	0.0170	0.001
k_{61} (min^{-1})	9.0×10^{-5}	2.81×10^{-5}
V_{PB} (ml/kg)	183	28
Vmax (μg/kg/min)	242	26
Km (μg/ml)	23.3	6.4
V_{PA} (ml/kg)	337	29
k_{25} (min^{-1})	2.1×10^{-7}	2.0×10^{-8}
k_{30} (min^{-1})	0.0940	0.03
k_{41} (min^{-1})	0.0057	0.0006
k_{52} (min^{-1})	0.0133	0.0013
V_{PAG} (ml/kg)	73	22

slow transfer from the peripheral to the central compartment (i.e. small k_{61} compared with k_{16}), is unclear. The volumes derived for PB, PA, and PAG, and the Vmax and Km for PA metabolism, are in good agreement with those previously reported for PB and PA studied separately [1, 22].

Discussion

PA and PB penetrated well into the CSF after i.v. administration. The half-lives of both PA and PB were somewhat longer in CSF than in plasma, resulting in a relatively high CSF exposure to the drugs with an AUC_{CSF}:AUC_{plasma} ratio of $28 \pm 19\%$ for PA and $41 \pm 47\%$ for PB. The elimination of PA from plasma and the CSF was essentially identical whether PA was administered i.v. or formed as a metabolite of PB. After administration of PB, ongoing formation of PA resulted in a twofold higher exposure in both plasma and CSF to PA than to PB. This result differs from that seen in a phase I study of adults with refractory solid tumors [1]. In that study, rapid metabolism of PA to its inactive metabolite PAG resulted in low exposures to PA relative to PB. However, the doses (600–2000 mg/m^2, approximately 15–60 mg/kg) were considerably lower than the PB dose of 130 mg/kg we used. In our study, PA concentrations after PB administration exceeded for several hours the published Km of 105 μg/ml for conversion of PA to PAG [22]. Although PB concentrations in our study also initially exceeded the Km for conversion of PB to PA (34 μg/ml) [1], PB concentrations fell below the Km before PA concentrations did. Thus the more than twofold higher exposure to PA than to PB in our study is readily explained by the prolonged period after PB administration during which PA concentrations exceeded the Michaelis-Menten rate constant for elimination of PA.

For the same reasons, the pharmacokinetic model that best describes our data includes a linear rate constant to describe the metabolism of PB to PA, but a capacity-limited (Michaelis-Menten) process to describe the metabolism of PA to PAG. It is likely that a different model would be more appropriate if much higher or lower drug doses had been administered. Similarly, although we report clearance values (i.e. dose/AUC) for PA, different clearances would be expected for different doses in a capacity-limited system. In addition, if there were differences in the metabolic pathways between Rhesus monkeys and humans, or polymorphisms in human enzymes responsible for metabolism of PA and PB, differences in the results between animal and human studies or between different human populations could occur. These considerations illustrate the complexity of PB and PA pharmacokinetics and emphasize the need for careful consideration of capacity-limited processes when extrapolating results from one dose or study to another.

Our results show good CSF penetration of PA and PB in the nonhuman primate. Significant CSF PA

concentrations have been also detected in two patients studied at single time-points after systemic PA administration [22]. This high CSF penetration has important clinical implications. PA and PB increase the sensitivity of HT20 colon carcinoma cells, MCF7 breast carcinoma cells, and U87 glioblastoma multiforme cells to radiation after 72-h exposures in vitro, possibly due to a decrease in intracellular antioxidant activity [24]. Since radiation is the primary therapeutic modality in many brain tumors, PA or PB could have a role in radiation sensitization in CNS malignancies. In addition, PB induces differentiation in medulloblastoma cell lines in vitro [25], another indication that its excellent CSF penetration may be clinically important.

The single-agent activity of PA and PB is unclear. In one study of PA in adults with recurrent malignant glioma, the response rate was less than 10% [26]. However, PA and PB may have important interactions with other anticancer agents. For example, PA and PB are synergistic against lymphoma cell lines in vitro with topotecan and cytarabine [27]. The CSF penetration of topotecan exceeds 30% [28], and cytarabine also penetrates into the CSF to a variable degree depending on the dose and schedule of administration [29, 30]. Thus PA or PB may have a role in combination with topotecan and cytarabine against meningeal lymphoma or other malignancies.

PA and PB are currently being studied in clinical trials. The high CSF penetration of these agents suggests that their activity in brain tumors, and especially in meningeal malignancy, should be evaluated. Administration of PB rather than PA might be advantageous, since PB administration results in exposure in plasma and CSF to both active compounds.

References

1. Piscitelli S, Thibault A, Figg W, Tompkins A, Headlee D, Lieberman R, Samid D, Myers C (1995) Disposition of phenylbutyrate and its metabolites, phenylacetate and phenylacetylglutamine. J Clin Pharmacol 35:368–373
2. Sandler M, Ruthven C, Goodwin B, Lee A, Stern G (1982) Phenylacetic acid in human body fluids: high correlation between plasma and cerebrospinal fluid concentration values. J Neurol Neurosurg Psychiatry 45:366–368
3. Moldave K, Meister A (1957) Synthesis of phenylacetylglutamine by human tissue. J Biol Chem 229:463–476
4. James J, Smith R, Williams F, Reidenberg M (1972) The conjugation of phenylacetic acid in man, sub-human primates and non-primate species. Proc R Soc Lond B Biol Sci 182:25–35
5. Brusilow S, Danney M, Waber L, Batshaw M, Burton B, Levitsky L, Roth K, Mckeethren C, Ward J (1984) Treatment of episodic hyperammonemia in children with inborn errors of urea synthesis. N Engl J Med 310:1630–1634
6. Simell O, Sipila I, Rajante J, Valle D, Brusilow S (1986) Waste nitrogen excretion via amino acid acetylation: benzoate and phenylacetate in lysinuric protein intolerance. Ped Res 20:1117–1121
7. Ram Z, Samid D, Walbridge S, Oshiro E, Viola J, Tao-Cheng J-H, Shack S, Thibault A, Myers C, Oldfield E (1994) Growth inhibition, tumor maturation, and extended survival in experimental brain tumors in rats treated with phenylacetate. Cancer Res 54:2923–2937
8. Samid D, Shack S, Sherman L (1992) Phenylacetate: a novel nontoxic inducer of tumor cell differentiation. Cancer Res 52:1988–1992
9. Samid D, Shack S, Myers C (1993) Selective growth arrest and maturation of prostate cancer cells in vitro by nontoxic, pharmacological concentrations of phenylacetate. J Clin Invest 91:2288–2295
10. Samid D, Ram Z, Hudgins W, Shack S, Liu L, Walbridge S, Oldfield E, Myers C (1994) Selective activity of phenylacetate against malignant gliomas: resemblance to fetal brain damage in phenylketonuria. Cancer Res 54:891–895
11. Samid D, Yeh A, Prasanna P (1992) Induction of erythroid differentiation and fetal hemoglobin production in human leukemic cells treated with phenylacetate. Blood 80:1576–1581
12. Liu L, Shack S, Stetler-Stevenson W, Judgins W, Samid D (1994) Differentiation of cultured human melanoma cells induced by the aromatic fatty acids phenylacetate and phenylbutyrate. J Invest Dermatol 103:335–340
13. Sidell N, Wada R, Han G, Chang B, Shack S, Moore T, Samid D (1995) Phenylacetate synergizes with retinoic acid in inducing the differentiation of human neuroblastoma cells. Int J Cancer 60:507–514
14. Engelhard H, Homer R, Duncan H, Rozental J (1998) Inhibitory effects of phenylbutyrate on the proliferation, morphology, migration and invasiveness of malignant glioma cells. J Neurooncol 37:97–108
15. Melchior S, Brown L, Figg W, Quinn J, Santucci R, Brunner J, Thuroff J, Lange P, Vessella R (1999) Effects of phenylbutyrate on proliferation and apoptosis in human prostate cancer cells in vitro and in vivo. Int J Oncol 14:501–508
16. Melichar B, Ferrandina G, Verschraengen C, Loercher A, Abbruzzese J, Freedman R (1998) Growth inhibitory effects of aromatic fatty acids on ovarian tumor cell lines. Clin Cancer Res 4:3069–3076
17. Shack S, Miller A, Liu L, Prasanna P, Thibault A, Samid D (1996) Vulnerability of multi-drug resistant tumor cells to the aromatic fatty acids phenylacetate and phenylbutyrate. Clin Cancer Res 2:865–872
18. Lea M, Tulsyan N (1995) Discordant effects of butyrate analogues on erythroleukemia cell proliferation, differentiation and histone deacetylase. Anticancer Res 15:879–883
19. Warrell R, He L, Richon V, Calleja E, Pandolfi P (1998) Therapeutic targeting of transcription in acute promyelocytic leukemia by use of an inhibitor of histone deacetylase. J Natl Cancer Inst 90:1621–1625
20. McCully C, Balis F, Bacher J, Phillips J, Poplack D (1990) A rhesus monkey model for continuous infusion of drugs into cerebrospinal fluid. Lab Anim Sci 40:522–525
21. National Research Council (1996) Guide for the care and use of laboratory animals. National Academy Press, Washington DC
22. Thibault A, Cooper M, Figg W, Venzon D, Sartor A, Tompkins A, Weinberger M, Headlee D, McCall N, Samid D, Myers C (1994) A phase I and pharmacokinetic study of intravenous phenylacetate in patients with cancer. Cancer Res 54: 1690–1694
23. Knott G (1979) MLAB: a mathematical modeling tool. Comput Programs Biomed 10:271–280
24. Miller A, Whittaker T, Thibault A, Samid D (1997) Modulation of radiation response of human tumour cells by the differentiation inducers, phenylacetate and phenylbutyrate. Int J Radiat Biol 1997 72:211–218
25. Lau C, Parikh S, Li X, Chow C, Jung H, Blaney S (1998) Differentiation induction in medulloblastoma cell lines by phenylbutyrate. Proc Am Assoc Cancer Res 39:108
26. Chang S, Kuhn J, Robins H, Schold A, Spence A, Berger M, Mehta M, Bozik M, Pollack I, Schiff D, Gilbert M, Rankin C, Prados M (1999) Phase II study of phenylacetate in patients with recurrent malignant glioma: a North American Brain Tumor Consortium Report. J Clin Oncol 17:984–990

27. Witzig T, Timm M, Svingen P, Kaufmann S (2000) Induction of apoptosis in malignant B cells by phenylbutyrate or phenylacetate in combination with chemotherapeutic agents. Clin Cancer Res 6:681–692
28. Blaney S, Cole D, Balis F, Godwin K, Poplack D (1993) Plasma and cerebrospinal fluid pharmacokinetic study of topotecan in nonhuman primates. Cancer Res 53:725–727
29. Donehower R, Karp J, Burke P (1986) Pharmacology and toxicity of high-dose cytarabine by 72-hour continuous infusion. Cancer Treat Rep 70:1059–1065
30. Lopez J, Nassif E, Vannicola P, Krikorian J, Agarwal R (1985) Central nervous system pharmacokinetics of high-dose cytosine arabinoside. J Neurooncol 3:119–124